

# Cost-effective CFD simulation to predict the performance of a hydrokinetic turbine farm

**O Pacot, D Pettinaroli, J Decaix and C Münch-Alligné**

University of Applied Sciences and Arts Western Switzerland, 1950 Sion, Switzerland

E-mail: [olivier.pacot@hevs.ch](mailto:olivier.pacot@hevs.ch)

**Abstract.** After the performance assessment of a new hydrokinetic turbine prototype in the tailrace channel of a run-of-river power plant (Lavey, CH), the possibility to install a farm of such hydrokinetic turbines on this pilot site is investigated. In order to identify the optimal number and size of the machines as well as their location on this site, numerical simulations are carried out. Such a process requires to simulate a set of several free surface flow computations including different configurations of the farm in order to maximize the energy tapped by the machines. However, free surface flow computations are time and resources consuming. To allow such flow investigations, a different approach has been selected. In the present study, the turbines were replaced by a model mimicking the resistance effect of the machines. This model consists in a pressure drop applied at the turbine location to emulate the disturbance effect on the flow, especially the wake effect that will modify the available kinetic energy for the neighboring machines. Finally, it results that such a low CPU approach allows us to estimate the best location of the hydrokinetic turbines maximizing the energy harvested.

## 1. Introduction

Our fast changing climate imposes us to tackle seriously the energy production issue. To do so, it is primordial, on one hand, to decrease our dependence to the electrical power and, on the other hand, to develop new efficient technologies to replace the existing ones. In this context, the plan in Europe is to start in the near future to dismantle the aging nuclear power plants and to replace them with environmental friendlier technologies as solar, wind or hydropower. However, the stakes of this transition are still significant and some challenges will have to be tackled as for example the low energy density of solar and wind energies and the difficulty to predict the availability of these resources. In Switzerland, the total electrical production of electricity by renewable energy reached approximately 40'000 GWh in 2017 (63.6% of the total electrical production) [1], of which, Small Hydro Powerplants (< 10MW), SHP, contributed to 10% approximately [2]. In addition, it is estimated that the SHP market has a potential growth of 1'600 GWh (+40%), which requires the development of new technologies to harvest this energy [3]. The great advantage of this hydraulic energy is that the electrical production is predictable and controllable, as the amount of water in lakes or flowing in rivers is already well documented or easily measurable. To meet this need to harvest the hydraulic energy of free surface and shallow flows, axial or vertical axis hydrokinetic turbines are developed [4, 5], featuring an electrical power output in the order of magnitude of a few kW to several hundred of kW. To reach an installed capacity of several MW, researches are ongoing to assemble these hydrokinetic turbines in an array, [6, 7, 8], requiring the study of the influence that a single



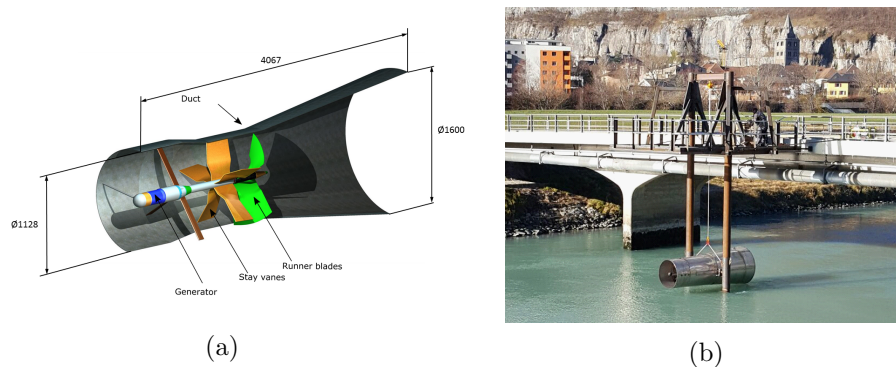


Figure 1: (a) Sketch of the kinetic turbine prototype along with main characteristic lengths (lengths in mm), (b) Open-air platform built in the Lavey tailrace channel

hydrokinetic turbine has on the performance of the other ones. Therefore, one of the main focus are on the position of the hydrokinetic turbine in the flow and on its wake recovery. However, such studies are very computationally expensive as it requires to simulate the flow field in the entire river as well as within the hydrokinetic turbine. To reduce the computational cost, the present paper introduces a methodology to simulate and predict the performance of a hydrokinetic turbine farm. The methodology can be decomposed into two main steps. First, a single hydrokinetic is studied numerically to establish the values of the resistance coefficient  $K$  versus the Tip Speed Ratio  $\lambda$  (TSR). Secondly, the flow within an entire farm is simulated using a turbine model relying on the previous resistance coefficient. Such turbine model reduces significantly the mesh requirement in the runner area and no rotating interfaces have to be computed in the simulation, which results in a gain of time and storage space.

## 2. Methodology

### 2.1. Hydrokinetic turbine prototype

The new prototype of a hydrokinetic turbine, shown in Fig. 1(a), was developed and built between the HES-SO Valais-Wallis and Stahleinbau GmbH<sup>1</sup> in Switzerland. This prototype consists in a small horizontal axis turbine, featuring four main components: the generator, the stay vanes, the runner and the duct. The latter allowing us to get rid of the Betz limit [9] and to accelerate the flow passing through the runner by the Venturi effect. The designed electrical power output is 1 kW. To test the prototype in real conditions, an open-air platform was built, shown in Fig. 1(b), and installed in the Lavey run-of-river hydropower plant's tailrace channel, located in the Western side of Switzerland on the Rhône River. The performances of the prototype were measured for several flow conditions: changes in the discharge, changes in the prototype depths and all this for several pitch angle of the prototype [10]. These measurement campaigns confirmed the expected performance obtained numerically by CFD and the measured power coefficient reached was higher than 80% for a maximal electrical power output of 1.4 kW. To increase the power installed, the prototype will be assembled with other prototypes to form a farm as shown in Fig. 2.

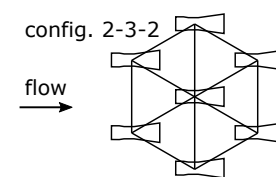


Figure 2: Farm configuration with 7 hydrokinetic turbines

<sup>1</sup> <https://www.stahleinbau.ch/>

## 2.2. Turbine model

To simplify the numerical simulation, the runner is replaced by a model eliminating the need of a fine grid around the runner blades as well as the interfaces between the rotating and stationary parts. For such a modeling, different approaches exist as the actuator disk or the blade element method [11]. These models cannot represent properly the physics taking place in the runner area and in the near wake, but can approximate fairly well the far wake region. In addition to the previous models, another one can be used, which mimics the pressure drop extracted by the runner. The advantage of this model is that the setup is simpler, i.e. no need to build a specific mesh to insert the actuator disk, it is more flexible as only parameters need to be changed and the fewer number of elements required reduces the computation time. Therefore, this model is selected for the present study. To apply a pressure drop at the runner location, a source term is added in the Navier-Stokes equations and is expressed as follow:  $S_i = K \rho U_i |U_i| / (2\Delta x)$ , where  $K$  is the resistance coefficient,  $\Delta x$  the distance on which the source term is applied,  $\rho$  the water density and  $U_i$  a component of the velocity vector. As it can be seen, the velocity component is part of the solution, but the resistance coefficient is a parameter of the simulation and may be thought of as a "pressure gradient per dynamic head" [12]. Figure 3 schematizes the methodology followed in this study.

## 2.3. Numerical setup

**2.3.1. Computational domains** To simulate the flow within a single prototype or a farm, two different computational domains are used, see Fig. 4. The physical dimensions were normalized using the runner diameter  $D$ . The location of the single prototype in the computational domain is located at  $x/D=4$  and  $z/D=3$ . Regarding the farm, see Fig. 2 (left), the first row is located at  $x/D=40$  and  $z/D=2.6$ .  $x/D=0$  being the inlet of the computational domain and  $z/D=0$  the river bed. The distances separating the prototypes in the farm are  $\Delta x/D = 5$  and  $\Delta y/D = 5$ .

**2.3.2. Meshes** Three different meshes were designed using ANSYS ICEM CFD. The first mesh (case 1), discretizing the rectangular subdomain, see Fig.4 (left), is unstructured and composed of 0.1 million tetrahedral elements. The second (case 2) and third meshes (case 3), both discretized the trapezoidal shape domain, see Fig.4 (right). The second mesh is unstructured and composed of 45.6 million tetrahedral elements. It includes the entire geometry of the seven prototypes. For the third mesh (case 3), a block structured mesh is used to minimize the amount of elements and is composed of 2.9 million rectangular elements. In this case, only the geometry of the duct

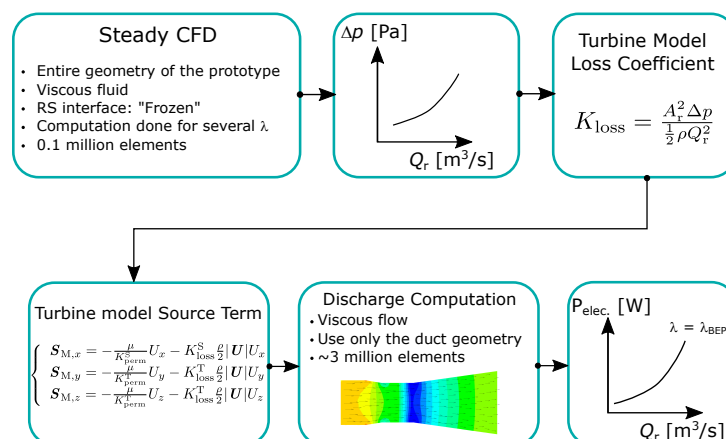


Figure 3: Flow chart of the present methodology

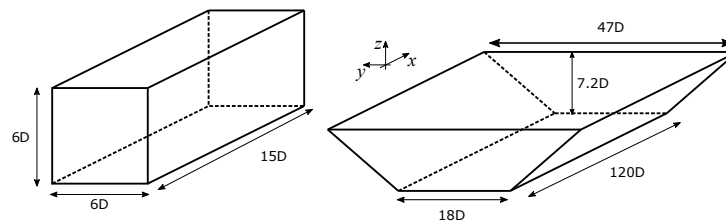


Figure 4: Computational domain used to simulate the flow through a single prototype (left) and in the flow through a farm (right). The dimensions are normalized by the runner diameter  $D$

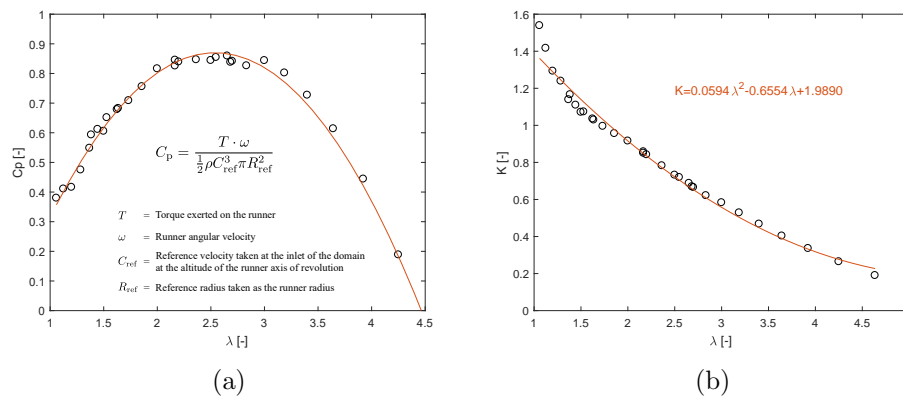


Figure 5: Power coefficient  $C_p$  (a) and coefficient of resistance  $K$  (b) computed for a single prototype at different tip speed ratio  $\lambda$

is taken into account, the runner being modeled resulting in a mesh 94% smaller compared to case 2.

**2.3.3. Boundary & running conditions** For steady simulations involving the single prototype the boundary conditions were set as follows: inlet: uniform velocity, wall: non-slip condition, outlet: average static pressure. The turbulence model was the  $k-\omega$  SST and the computation used the Frozen Rotor interface. For unsteady computations involving the farm, the free surface was taken into account with the CFX free surface model. The inlet was set using a velocity profile following a  $1/7$  power law. The outlet was an opening, walls were set to non-slip condition. For the computation of case 2, the turbulence model was the  $k-\omega$  SST and for the case 3 the  $k-\epsilon$  was selected. The time step size corresponded to a  $4^\circ$  rotation of the runner for case 2 and was set to 0.5 [s] for case 3. All computations were performed using ANSYS CFX R17.2.

### 3. Results

#### 3.1. Performance of a single hydrokinetic turbine

The flow field passing in a single prototype was computed for several combination of the tip speed ration  $\lambda$  to establish the performance characteristic of the hydrokinetic turbine. Each computation took approximately 24 CPU hours using a Dual Intel Xeon X5650 (12 cores, 24 GB of RAM) and reached a RMS residual level around  $10^{-4}$ . The results obtained are shown in Fig. 5(a), where the best efficiency point reached a  $C_p = 0.87$  [-] corresponding to a  $\lambda=2.54$  [-]. Based on these simulations, the coefficient of resistance  $K$  can be computed, see Fig. 5(b). These results will be used in the following to set the parameters of the turbine model, i.e. at the best efficiency point, the corresponding  $K=0.71$  [-].

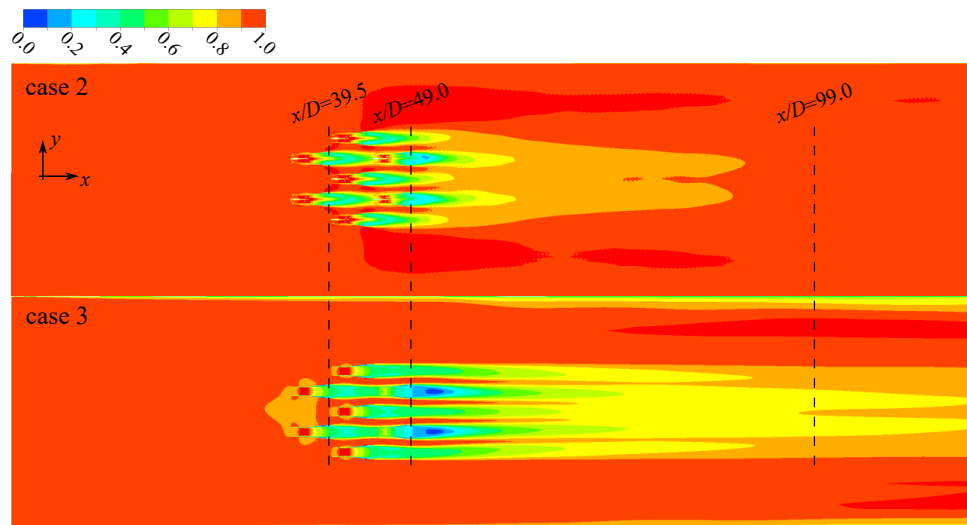


Figure 6: Comparison of the instantaneous normalized streamwise velocity on the  $Oxy$  plane ( $z/D=2.6$ )

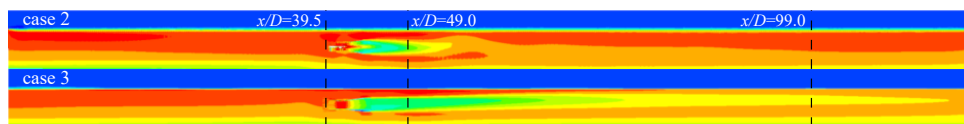


Figure 7: Comparison of the instantaneous normalized streamwise velocity on the  $Ozx$  plane ( $y/D=0.0$ )

### 3.2. Flow comparison of cases 2 & 3

The flow field passing through the farm composed of seven prototypes were computed both for case 2 and case 3. It required approximately 25'000 CPU hours to simulate the case 2 using a Dual Intel Xeon E5-2699 v4 (44 cores, 128 GB of RAM) and approximately 1'500 CPU hours to simulate the case 3 using a Dual Intel Xeon E5-2690 v3 (24 cores, 64 GB of RAM), which resulted in a gain of CPU hour of 93%. Their instantaneous normalized streamwise distributions of the velocity on plane  $Oxy$  at  $z/D=2.6$  are given in Fig. 6. It can be seen that the wake recovers faster in case 2 compared to case 3. Several reasons may explain this behavior. One is that in case 2, the flow passing through the turbine enters into rotation and will swirl downstream the prototype. This phenomenon will accelerate the momentum transfer and increase the wake recovery process. Another reason is because of the mesh type. Case 2 uses a fine unstructured mesh, whereas case 3 uses a coarser structured mesh, which is well aligned with the flow. Despite both computation are using the high resolution scheme, it still might be more difficult for the structure mesh to resolve the lateral convective and diffusive fluxes. It results that the high velocity jet passing in between the prototypes expands up to  $10D$  downstream the last row of the farm in case 3, whereas it is only approximately  $2D$  for case 2. The vertical distribution of the instantaneous normalized streamwise velocity on plane  $Ozx$  ( $y/D=0.0$ ) is shown in Fig. 7. The wake in case 2 exhibits a more axial symmetry, which is probably due to the rotation effect. For case 3, the maximum velocity deficit is first located near the channel bed. Further downstream, the interaction with the bed boundary layer will move the velocity deficit toward the free surface. The instantaneous normalized horizontal and vertical velocity profiles at  $x/D=39.5$  and  $99.0$  are shown in Fig. 8. The profiles at  $x/D=39.5$  for case 2 and 3 are very close. At  $x/D=99.0$ , the mean velocity between  $y/D=[-4\ 4]$ , see Fig. 8(a) right, reach 0.91 and 0.79 for case 2 and case

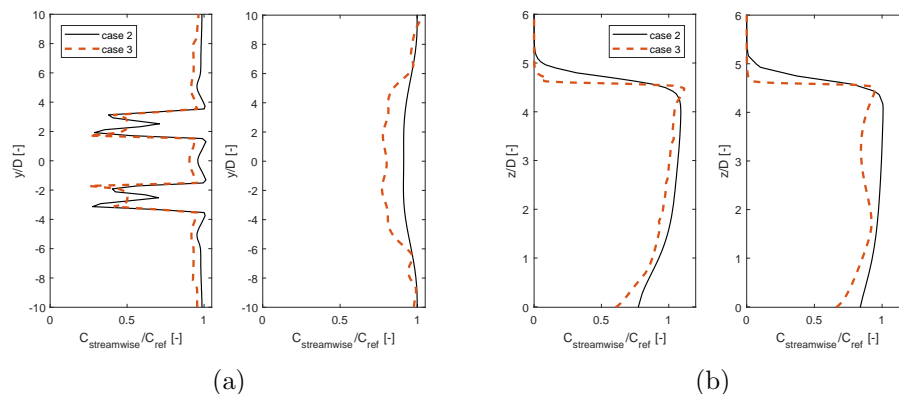


Figure 8: Comparison of the instantaneous normalized velocity profiles. (a) horizontal profile at  $z/D=2.6$ . Left:  $x/D=39.5$ . Right:  $x/D=99.0$ . (b) vertical profile at  $y/D=0.0$ . Left:  $x/D=39.5$ . Right:  $x/D=99.0$

3, respectively. The lack of flow rotation in case 3 makes the wake recovery process longer. However, the difference is only of -13%, which is considered acceptable for the objective of this study. Similarly, the vertical profile, see Fig. 8(b) right, still exhibits the velocity deficit due to the wake. The maximum deficit is located  $0.6D$  higher than the turbine axis location.

#### 4. Conclusion

A methodology was proposed to investigate at lower cost the flow field past a hydrokinetic farm to predict the performance of another hydrokinetic farm located downstream the first farm. The methodology relies on a turbine model that mimic the pressure drop within the runner area without the need to compute accurately the flow field around the blades and at the interfaces between rotating and stationary parts. It was shown that the computed far wake velocity was only 13% lower compared to a fully transient computation using a mesh of 45 million of tetrahedral elements. Furthermore, the use of the turbine model resulted in a mesh 94% smaller than the fully transient mesh and requiring approximately 16 times less CPU hour. Therefore, this methodology is well suited for an initial investigation on where to place hydrokinetic turbines in a river to get the maximum power output.

#### 5. Acknowledgments

The authors would like to thank the SCCER SoE, the Swiss Federal Office of Energy, The Ark Foundation and Services Industriels de Lausanne for their financial support.

#### 6. References

- [1] OFS 2018 Production d'électricité - 1970-2017 URL <https://www.bfs.admin.ch>
- [2] SSH 2018 Importance de la petite centrale hydraulique URL <https://swissmallhydro.ch>
- [3] OFEN 2012 Le potentiel hydroélectrique de la Suisse Tech. rep. Office fédéral de l'énergie Bern
- [4] Khan M, Bhuyan G, Iqbal M and Quaicoe J 2009 *Applied Energy* **86** 1823–1835
- [5] Laws N D and Epps B P 2016 *Renewable and Sustainable Energy Reviews* **57** 1245–1259
- [6] Bahaj A and Myers L 2013 *Energy* **59** 83–94
- [7] Birjandi A H, Bibeau E L, Chatoorgoon V and Kumar A 2013 *Ocean Engineering* **69** 9–17
- [8] Riglin J, Daskiran C, Jonas J, Schleicher W C and Oztekin A 2016 *Renewable Energy* **97** 274–283
- [9] Betz A 1966 *Introduction to the theory of flow machines* (Pergamon Press)
- [10] Münch-Alligné C, Schmid J, Richard S, Gaspoz A, Brunner N and Hasmatuchi V 2018 *Water* **10** 311
- [11] Batten W M J, Harrison M E and Bahaj A S 2013 *Phil Trans R Soc A* **371** 20120293–20120293
- [12] ANSYS *ANSYS CFX Theory Guide* Ansys Inc.